Inorg. Chem. **2009**, *48*, 2364−2370

Solvent-Assisted Formation of Vesicles by a Self-Assembling Ni_3−Schiff Base Complex

Pampa Mukherjee,[†] Michael G. B. Drew,[‡] and Ashutosh Ghosh*[,†]

Department of Chemistry, University College of Science, University of Calcutta, 92, A.P.C. Road, Kolkata-700 009, India, and School of Chemistry, The University of Reading, P. O. Box 224, Whiteknights, Reading RG 66AD, United Kingdom

Received May 21, 2008

A linear trinuclear Ni−Schiff base complex $[Ni_3(salpen)_2(PhCH_2COO)_2(EtOH)]$ has been synthesized by combining $Ni(ClO_4)_2 \cdot 6H_2O$, phenyl acetic acid ($C_6H_5CH_2COOH$), and the Schiff base ligand, N,N′-bis(salicylidene)-1,3-pentanediamine (H_2salpen). This complex is self-assembled through hydrogen bonding and C−H−π interaction in the solid state to generate a sheet-like architecture, while in organic solvent (CH_2Cl_2), it forms vesicles with a mean diameter of 290 nm and fused vesicles, depending upon the concentration of the solution. These vesicles act as an excellent carrier of dye molecules in CH_2Cl_2. The morphology of the complex has been determined by scanning electron microscopy and transmission electron microscopy experiments, and the encapsulation of dye has been examined by confocal microscopic image and electronic absorption spectra.

Introduction

Molecular self-assembly is a ubiquitous theme in natural systems where constituent building blocks are recruited following precise pairing patterns, to reveal an array of hierarchical architectures that are primarily supported by noncovalent interactions.[1,2] Over the years, various natural self-assembling systems have served as inspiration for the design of novel building blocks on the nanoscale. The rapidly growing research in controlling the size and morphology of nanostructured materials has created an increasing demand for supramolecular self-assemblies used as organized templates, which should be easily constructed in a highly reproducible way and with perfect control of the organized structures. A number of different organized assemblies, such as spherical,[3] rodlike or wormlike,[4] and disklike micelles;[5] flat lamellar bilayers;[3a,6] closed uni- and multilamellar vesicles;[7] and nanotubes,[8] have all been recently used to produce advanced nanostructured materials.[9] The main driving force for constructing such organized assemblies arises from weak van der Waals, hydrophobic, hydrogen-bonding, and screened electrostatic interactions and so forth.[10] The synthesis and study of nanometer-scaled assemblies have attracted a great deal of attention in recent years because of their fundamental interest and their potential applications in many fields, including electronics, catalysis, separation, biology, medical imagery, and others.[11] However, the synthesis of such nanosized objects is rendered difficult because of the need of size, shape, phase purity, and surface

* To whom correspondence should be addressed. E-mail: ghosh_59@yahoo.com.
[†] University of Calcutta.
[‡] The University of Reading.

(1) Lehn, J. M. *Science* **2002**, *295*, 2400–2403.
(2) Whitesides, G. M.; Grzybowski, B. *Science* **2002**, *295*, 2418–2421.
(3) (a) Wang, W.; Efrima, S.; Regev, O. *J. Phys. Chem. B* **1999**, *103*, 5613–5621. (b) Zhang, Z.; Patel, R. C.; Kothari, R.; Johnson, C. P.; Friberg, S. E.; Aikens, P. A. *J. Phys. Chem. B* **2000**, *104*, 1176–1182. (c) Brinker, C. J.; Lu, Y.; Sellinger, A.; Fan, H. *Adv. Mater.* **1999**, *11*, 579–585.
(4) Zhang, M.; Drechsler, M.; Müller, A. H. *Chem. Mater.* **2004**, *16*, 537–543. (b) Keller, S. L.; Boltenhagen, P.; Pine, D. J.; Zasadzinski, J. A. *Phys. Rev. Lett.* **1998**, *80*, 2725–2728.
(5) Zemb, Th.; Dubois, M.; Demé, B.; Gulik-Krzywicki, Th. *Science* **1999**, *283*, 816–819.
(6) Lee, B.; Luo, H.; Yuan, C. Y.; Lin, J. S.; Dai, S. *Chem. Commun.* **2004**, 240–241.
(7) Correa, N. M.; Zhang, H.; Schelly, Z. A. *J. Am. Chem. Soc.* **2000**, *122*, 6432–6434. (b) Pevzner, S.; Regev, O.; Lind, A.; Lindén, M. *J. Am. Chem. Soc.* **2003**, *125*, 652–653. (c) Hubert, D. H. W.; Jung, M.; German, A. L. *Adv. Mater.* **2000**, *12*, 1291–1294. (d) Kisak, E. T.; Coldren, B.; Zasadzinski, J. A. *Langmuir* **2002**, *18*, 284–288.
(8) Beck, R.; Abe, Y.; Terabayashi, T.; Hoffmann, H. J. *Phys. Chem. B* **2002**, *106*, 3335–3338. (b) Liu, T.; Burger, C.; Chu, B. *Prog. Polym. Sci.* **2003**, *28*, 5–26.
(9) Pileni, M. P. *Nat. Mater.* **2003**, *2*, 145–150. Also see the references in this review article.
(10) Israelachvili, J. N. *Intermolecular and Surface Forces*, 2nd ed.; Academic Press Ltd: New York, 1991.
(11) Feldheim, D. L.; Foss, C. A., Jr. *Metal Nanoparticles. Synthesis, Characterization, and Applications*; Marcel Dekker: New York, 2002.

10.1021/ic801889a CCC: $40.75
Published on Web 02/13/2009

state control. Among numerous investigated nanosized objects of different types, vesicles are relatively rare and important because of their potential application in the encapsulation, controlled release, and biological stability of bioactive compounds.[12] In previous works, vesicles based on small peptide molecules,[12a−c] amphiphilic block-copolymers,[12d−g] or other bio-inspired organic molecules[12h−j] have been observed by many scientists. Recently, some metal-ion-induced vesicle formation has also been observed.[12k−o] But organic-phase-soluble vesicles or fused vesicles based on the self-assembly of any transition metal complex have not been reported to date. Moreover, in previous works, the encapsulation properties of vesicles have been investigated mostly in the aqueous phase, and it almost remains unexplored in the organic phase.

Herein, we report a new phenyl acetate bridged trinuclear Ni(II)−Schiff base complex $[Ni_3(salpen)_2(PhCH_2COO)_2(EtOH)]$ (**1**) (salpen = N,N′-bis(salicylidene)-1,3-pentanediamine) which self-assembles to a sheet-like architecture in the solid state but in CH_2Cl_2 medium forms vesicles and fused vesicles, depending on the concentration of the solution. Moreover, encouraged by the preliminary observations, the possible effects of a solvent on the stability of vesicles have also been observed.

Experimental Section

Materials. The reagents and solvents used were of commercially available reagent quality, unless otherwise stated.

Synthesis of the Schiff Base N,N′-Bis(salicylidene)-1,3-pentanediamine (H_2salpen). The Schiff base was prepared by the condensation of salicylaldehyde (1.05 mL, 10 mmol) and 1,3-pentanediamine (0.596 mL, 5 mmol) in methanol (10 mL), as reported previously.[13]

Synthesis of Complex $[Ni_3(salpen)_2(PhCH_2COO)_2(EtOH)]$ (1). A solution of $Ni(ClO_4)_2\cdot 6H_2O$ (7.5 mmol, 2.742 g) in methanol (5 mL) was added to a solution of H_2salpen (5 mmol) in methanol (10 mL) followed by the addition of a methanol solution (10 mL) of $C_6H_5CH_2COOH$ (5 mmol, 0.680 g). Triethylamine (2.1 mL, 15 mmol) was added dropwise to this solution with constant stirring. Upon standing the mixture overnight in an open atmosphere, a green precipitate separated out. The green solid was then filtered off and washed with diethyl ether and then redissolved in CH_2Cl_2. Layering of the green solution with EtOH gave well-formed X-ray-quality green single crystals of **1**. Yield: 2.1 g, 70%. Anal. calcd for $C_{57}H_{57}Cl_2N_4Ni_3O_9$: C, 57.58; H, 4.83; N, 4.71%. Found: C, 57.40; H, 4.65; N, 4.55%. λ_{Max} (CH_2Cl_2): 617 and 358 nm. HRMS (ESI) found: m/z $(M + K)^+ = 1148.5248$; $M_{calcd} = 1109.14$.

Table 1. Crystal Data and Structure Refinement of Complex **1**

empirical formula	$C_{57}H_{57}Cl_2N_4Ni_3O_9$
fw	1194.14
space group	$P21/n$
cryst syst	monoclinic
a/Å	16.5093(14)
b/Å	15.8514(10)
c/Å	20.5452(19)
β/deg	91.135(8)
V/Å^3	5375.5(8)
Z, calculated density	4, 1.468
abs coeff (μ) mm^{-1}	1.200(Mo Kα)
F(000)	2484
cryst size	0.03 × 0.18 × 0.19
refinement method	SHELXL-97 on F^2
θ range for data collection	2.4 to 30.0 deg.
R (int)	0.173
no. of unique data	12714
no. of data with $I > 2\sigma(I)$	5187
R1, wR2	0.1328, 0.2491

Physical Measurements. Elemental analyses (C, H, and N) were performed using a Perkin-Elmer 240C elemental analyzer. IR spectra in KBr (4500−500 cm^{-1}) were recorded using a Perkin-Elmer RXI FT-IR spectrophotometer. The electronic absorption spectra (1200−350 nm) of the complexes were recorded in CH_2Cl_2 with a Hitachi U-3501 spectrophotometer. Scanning electron microscopy (SEM) experiments were performed using a VEGA II LSU electron microscope. Transmission electron microscopy (TEM) studies were carried out using a Tecnai 30ST electron microscope. A CH_2Cl_2 solution of complex **1** was taken at a concentration of 1 mg/mL, and a drop of that solution was taken in a carbon-coated copper grid (300 mesh) and evaporated to dryness under a vacuum for 2 days. With these grids, the TEM study was carried out. Atomic force microscopy (AFM) was performed using an AUTOPROBE CP BASE UNIT di CP-II instrument, model number AP-0100. A dynamic light scattering (DLS) experiment was performed using a Malvern instruments zeta sizer, Nano Series, Nano ZS, and a confocal microscopic analysis was performed using a Leica Confocal microscope, TCS SP2. X-ray photoelectron spectra (XPS) were recorded with an ESCALAB MKIV spectrometer employing Al Kα radiation (1486.6 eV). The spectra have been corrected with respect to the graphitic carbon core-level peak (B.E. 284.6 eV) due to charging and other effects. High-resolution mass spectra (HRMS-ESI) were recorded on a Qtof Micro YA263 high-resolution mass spectrometer. For HRMS-ESI, the sample was taken in CH_2Cl_2.

Crystal Data Collection and Refinement. Crystal data for complex **1** are given in Table 1. A total of 12 714 points of independent data were collected with Mo Kα radiation using the Oxford Diffraction X-Calibur CCD System. The crystals were positioned at 50 mm from the CCD. A total of 321 frames were measured with a counting time of 10 s. Data analysis was carried out using the Crysalis program.[14] The structures were solved using direct methods with the Shelx97 program.[15] The non-hydrogen atoms were refined with anisotropic thermal parameters. The hydrogen atoms bonded to carbon were included in geometric positions and given thermal parameters equivalent to 1.2 times those of the atom to which they were attached. Empirical absorption

(12) (a) Reches, M.; Gazit, E. *Nano Lett.* **2004**, *4*, 581–585. (b) Ghosh, S.; Reches, M.; Gazit, E.; Verma, S. *Angew. Chem., Int. Ed.* **2007**, *46*, 2002–2004. (c) Mishra, A.; Panda, J.; Basu, A.; Chauhan, V. S. *Langmuir* **2008**, *24*, 4571–4576. (d) Tian, L.; Nguyen, P.; Hammond, T. *Chem. Commun.* **2006**, 3489–3491. (e) Gao, K.-J.; Li, G.; Lu, X.; Wu, Y. G.; Xua, B. P.-Q.; Fuhrhop, J.-H. *Chem. Commun.* **2008**, 1449–1451. (f) Vriezema, D. M.; Hoogboom, J.; Velonia, K.; Takazawa, K.; Christianen, P. C. M.; Maan, J. C.; Rowan, A. E.; Nolte, R. J. M. *Angew. Chem., Int. Ed.* **2003**, *42*, 772–776. (g) Joshi, K. B.; Verma, S. *Angew. Chem., Int. Ed.* **2008**, *47*, 1–5. (h) Soman, N. R.; Lanza, G. M.; Heuser, J. M.; Schlesinger, P. H.; Wickline, S. A. *Nano Lett.* **2008**, *8*, 1131–1136. (i) Ajayaghosh, A.; Chithra, P.; Varghese, R. *Angew. Chem., Int. Ed.* **2007**, *46*, 230–233. (j) Ajayaghosh, A.; Varghese, R.; Mahesh, S.; Praveen, V. K. *Angew. Chem., Int. Ed.* **2006**, *45*, 7729–7732. (k) Luo, X.; Wu, S.; Liang, Y. *Chem. Commun.* **2002**, 492–493. (l) Charvet, R.; Jiang, D.-L.; Aida, T. *Chem. Commun.* **2004**, 2664–2665. (m) Constable, E. C.; Meier, W.; Nardin, C.; Mundwiler, S. *Chem. Commun.* **1999**, 1483–1484. (n) Richard, A.; Artzner, V. M.; Lalloz, M. N.; Brienne, M.-J.; Artzner, F.; Krzywicki, T. G.; Boudeville, M. A. G.; Lehn, J.-M. *Proc. Natl. Acad. Sci. U. S. A.* **2004**, *101*, 15279–15284. (o) Hemakanthi, G.; Dhathathreyan, A. *J. Colloid Interface Sci.* **2002**, *253*, 393–396.

(13) Mukherjee, P.; Biswas, C.; Drew, M. G. B.; Ghosh, A. *Polyhedron* **2007**, *26*, 3121–3128.

(14) *Crysalis*, v.1; Oxford Diffraction Ltd.: Oxford, U.K., 2005.

(15) Sheldrick, G. M. *SHELXL-97*; University of Göttingen: Göttingen, Germany, 1997.

corrections were carried out using the ABSPACK program.[16] The structures were refined on F2 using Shelx97[15] to R1 = 0.1325 and wR2 = 0.2055 for 5187 reflections with $I > 2\sigma(I)$.

Results and Discussion

The addition of a methanol solution of $Ni(ClO_4)_2 \cdot 6H_2O$ to a methanol solution containing phenyl acetic acid ($C_6H_5CH_2COOH$) and the Schiff base ligand H_2salpen (N,N′-bis(salicylidene)-1,3-pentanediamine) followed by triethylamine results in a green amorphous compound. When it is dissolved in CH_2Cl_2 and evaporated to dryness, a green sticky mass results. However, layering of the CH_2Cl_2 solution of the compound with EtOH yielded the well-formed X-ray-quality green single crystals of $[Ni_3(salpen)_2(PhCH_2COO)_2(EtOH)]$ (**1**). The trinuclear complex forms a supramolecular sheet-like structure in the solid state. Hence, our aim was to investigate the morphologies of the compound in both the solid and solution states (in CH_2Cl_2) and to correlate them. Interestingly, it has been found that this complex forms vesicular structures in CH_2Cl_2 that were visualized through TEM, SEM, and AFM. The size distribution of the vesicles has been observed in DLS experiments. The molecular ion peak position in HRMS-ESI in CH_2Cl_2 ensures that the Ni_3 complex was retained even after vesicle formation (Figure S1, Supporting Information). Moreover, the XPS analysis of the complex in vesicular form (obtained from CH_2Cl_2) and in crystalline form (obtained by the slow diffusion of CH_3CH_2OH into a CH_2Cl_2 solution of complex **1**) showed nearly identical spectra with main signals of the Ni $2p_{3/2}$ and $2p_{1/2}$ peaks at 853.6 and 872.1 eV, respectively (Figures S2 and S3, Supporting Information). The spectra also indicate identical peak positions for C, N, and O (Figure S4, Supporting Information). The results undoubtedly confirm the presence of the identical structure in both the crystalline and vesicular states having octahedral Ni(II).[17]

It is also to be mentioned that complex **1** is precipitated out on the addition of CH_3CN or C_2H_5OH to its saturated CH_2Cl_2 solution. Moreover, the single crystal of **1** was obtained by slow diffusion of C_2H_5OH to its solution in CH_2Cl_2. These observations clearly exclude the possibility of the breaking up of the polynuclear structure of the complex species on the addition of good donor solvents.

IR and UV−Vis Spectra of Complexes. In the IR spectra of complex **1**, a strong and sharp band due to azomethine υ(C═N) appears at 1626 cm^{-1}. The attributions of the IR spectra in the 1300−1600 cm^{-1} region are difficult due to the appearance of several absorption bands from both the Schiff base ligand and phenyl acetate. The strong bands at 1585 cm^{-1} with a shoulder at 1626 cm^{-1} are likely due to the overlapping of bands from Schiff bases with the antisymmetric stretching mode of the carboxylate group.[18]

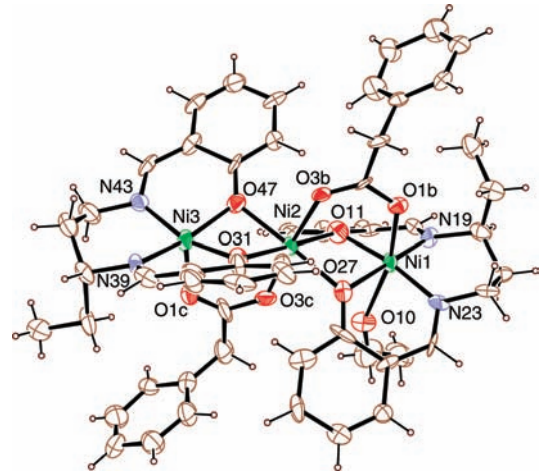

Figure 1. ORTEP-3 view of the asymmetric unit of **1** with ellipsoids at 50% probability (CH_2Cl_2 is omitted for clarity).

The shoulders at 1626 cm^{-1} may be attributed to the ν_a(CO) of the $PhCH_2COO^-$ group, and the symmetric stretching modes for the carboxylate are observed at 1400 cm^{-1}.

The electronic absorption spectra of complex **1** are recorded in CH_2Cl_2 (where vesicular structures are formed), and also in a CH_2Cl_2/CH_3CH_2OH solvent mixture (where vesicular structures are not formed, instead a crystalline product was obtained by the slow diffusion of a CH_2Cl_2 solution of the complex into CH_3CH_2OH; Figure S5, Supporting Information). The spectra in these two mediums are very similar, showing a broad band near about 930 nm, well-separated from the second transition near 570 nm, as is usual for octahedral Ni(II).[19] The higher-energy d−d bands are obscured by strong charge-transfer transitions. The very similar spectra of the compound in these two solvent systems indirectly prove that the trinuclear structure of the compound is retained in CH_2Cl_2 solution and also in vesicle walls.

Description of the Structure of $[Ni_3(salpen)_2(PhCH_2COO)_2(EtOH)]$ (1). The crystal structure of **1** is comprised of a discrete trimeric unit of the neutral compound $[Ni_3(salpen)_2(PhCH_2COO)_2(EtOH)]$ together with one solvent molecule of CH_2Cl_2. A labeled diagram is shown in Figure 1, and the selected bond lengths and angles are summarized in Table 2. In the trimeric structure, three nickel atoms are in an approximately linear disposition. The two tetradentate ligands are bound to the two outer nickel atoms. The central nickel atom, Ni(2), has a coordination number of six, being bonded to the four oxygen atoms of the two outer Ni(salpen) moieties at an average distance of 2.078 Å, which form the square plane of the Ni(II), while its trans axial positions are occupied by the bridging carboxylate oxygen atoms (O3b and O3c) of the phenyl acetate ligand at an average distance of 2.023 Å. The two outer nickel atoms, Ni(1) and Ni(3), are bonded to four atoms from the ligand salpen, making up the equatorial plane, with two oxygen atoms, O(11) at 1.959(5) Å and O(27) at 2.011(8) Å, two imine nitrogen atoms, N(19) at 1.990(10) Å and N(23) at 1.975(10) Å for Ni(1), atoms O(31) at 2.061(8) Å and O(47) at 2.087(8) Å,

(16) *ABSPACK*; Oxford Diffraction Ltd.: Oxford, U.K., 2005.
(17) (a) Matienzo, J.; Yin, L. I.; Grim, S. O.; Swartz, W. E. *Inorg. Chem.* **1973**, *12*, 2762–2769. (b) Li, Y.; Hao, N.; Lu, Y.; Wang, E.; Kang, Z.; Hu, C. *Inorg. Chem.* **2003**, *42*, 3119–3124. (c) Zhou, J.; Bian, G.-Q.; Zhang, Y.; Zhu, Q.-Y.; Li, C.-Y.; Dai, J. *Inorg. Chem.* **2007**, *46*, 6347–6352.
(18) Sarkar, B.; Drew, M. G. B.; Estrader, M.; Diaz, C.; Ghosh, A. *Polyhedron,* **2008**, *27*, 2625–2633, and the references cited therein.
(19) Mukherjee, P.; Drew, M. G. B.; Estrader, M.; Ghosh, A. *Inorg. Chem.* **2008**, *47*, 7784–7791.

Table 2. Selected Bond Lengths (Å) and Bond Angles (deg) for Complex **1**

Ni1−O1B	2.098(8)	O1B−Ni1−O10	166.5(3)	O3C−Ni2−O11	89.5(3)
Ni1−O10	2.365(9)	O1B−Ni1−O11	91.7(3)	O3C−Ni2−O27	88.2(3)
Ni1−O11	1.959(9)	O1B−Ni1−O27	88.7(3)	O3C−Ni2−O31	89.6(3)
Ni1−O27	2.011(8)	O1B−Ni1−N19	97.2(4)	O3C−Ni2−O47	90.7(3)
Ni1−N19	1.990(10)	O1B−Ni1−N23	96.0(4)	O11−Ni2−O27	81.9(3)
Ni1−N23	1.975(10)	O10−Ni1−O11	80.0(3)	O11−Ni2−O31	177.8(4)
Ni2−O3B	2.024(8)	O10−Ni1−O27	80.3(3)	O11−Ni2−O47	100.2(3)
Ni2−O3C	2.023(8)	O10−Ni1−N19	93.3(4)	O27−Ni2−O31	100.1(3)
Ni2−O11	2.069(9)	O10−Ni1−N23	91.4(4)	O27−Ni2−O47	177.6(3)
Ni2−O27	2.096(8)	O11−Ni1−O27	86.9(3)	O31−Ni2−O47	77.8(3)
Ni2−O31	2.061(8)	O11−Ni1−N19	89.0(4)	O1C−Ni3−O31	96.3(4)
Ni2−O47	2.087(8)	O11−Ni1−N23	170.6(4)	O1C−Ni3−O47	96.0(3)
Ni3−O1C	2.002(10)	O27−Ni1−N19	172.9(4)	O1C−Ni3−N39	99.9(4)
Ni3−O31	1.963(8)	O27−Ni1−N23	88.1(4)	O1C−Ni3−N43	98.4(4)
Ni3−O47	2.021(8)	N19−Ni1−N23	95.2(4)	O31−Ni3−O47	81.7(3)
Ni3−N39	1.983(9)	O3B−Ni2−O3C	174.5(3)	O31−Ni3−N39	92.2(4)
Ni3−N43	2.029(10)	O3B−Ni2−O11	87.5(3)	O31−Ni3−N43	162.8(4)
		O3B−Ni2−O27	86.8(3)	O47−Ni3−N39	163.5(4)
		O3B−Ni2−O31	93.5(3)	O47−Ni3−N43	88.0(4)
		O3B−Ni2−O47	94.5(3)	N39−Ni3−N43	94.0(4)

Table 3. Hydrogen-Bond Geometries in Compound **1** (in Å and deg)

D−H···A[a]	*d*(D−H)	*d*(D···A)	*d*(H···A)	>(D−H···A)
C1−H1B···O3B′	0.9700	3.248(17)	2.3300	157.00
C10C−H10C···O1B″	0.9300	3.404(15)	2.5000	163.00
C13−H13···O47″	0.9300	3.310(15)	2.5500	139.00
C201−H20B···O1B″	0.9700	3.279(15)	2.5100	136.00
C27−H27···O31″	0.9300	3.354(17)	2.5500	146.00
C33−H33···O27″	0.9300	3.308(15)	2.5800	136.00
C421−H42C···O1C″	0.9700	3.246(15)	2.4100	144.00
C47−H47···O11″	0.9300	3.294(15)	2.5800	134.00

[a] Symmetry code: ′ = (−1/2 + *x*, 1/2 − *y*, −1/2 + *z*), ″ = (1 − *x*, 1 − *y*, 2 − *z*).

and two imine nitrogen atoms, N(39) at 1.983(9) Å and N(43) at 2.029(10) Å, for Ni(3). Ni(1) and Ni(3) are axially coordinated by the oxygen atoms, O(1b) and O(1c), respectively, of phenyl acetate. Ni(1) is six-coordinate, being bonded weakly to a solvent ethanol molecule (Ni1−O10, 2.365 Å), while Ni(3) remains five-coordinate. For both the Ni atoms (Ni1 and Ni3), the four basal donor atoms are almost coplanar with respect to their mean planes, with a maximum deviation of 0.02 Å. The deviations of Ni(1) and Ni(3) are 0.123 and 0.270 Å from their respective mean planes toward the carboxylate oxygen atoms O(1b) and O(1c), respectively. In this complex, it seems unlikely that there is any interaction between the nickel atoms. The average Ni···Ni distance is 2.99 Å, with a Ni···Ni···Ni angle of 172°.

The complex self-assembles through several C−H···O hydrogen-bonding (Figure 2, Table 3) and C−H−π interactions (Figure S7, Table S1, Supporting Information) to form a supramolecular sheet structure in the solid state. Dichloromethane molecules being trapped inside this metal-organic framework help the formation and stabilization of such hydrogen-bonded sheet structures along the crystallographic

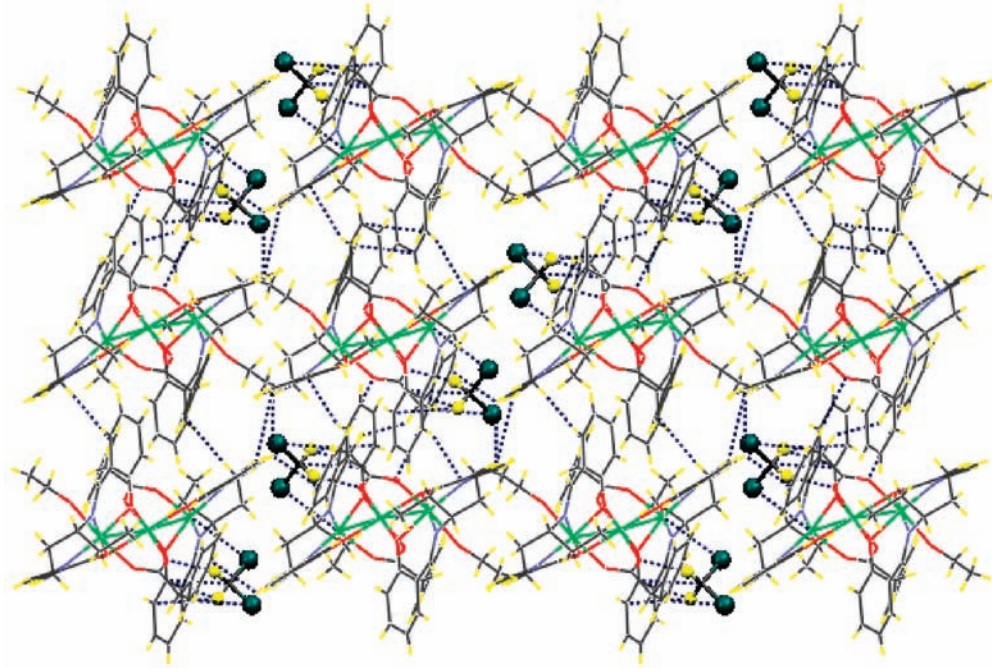

Figure 2. Hydrogen-bonded supramolecular sheet-like structure (along the crystallographic *b* axis) of complex **1**, obtained from single-crystal X-ray crystallography. Dotted lines indicate hydrogen bonds. Color code: red, oxygen; blue, nitrogen; gray, carbon; white, hydrogen; green, nickel; fluorescent green, chlorine.

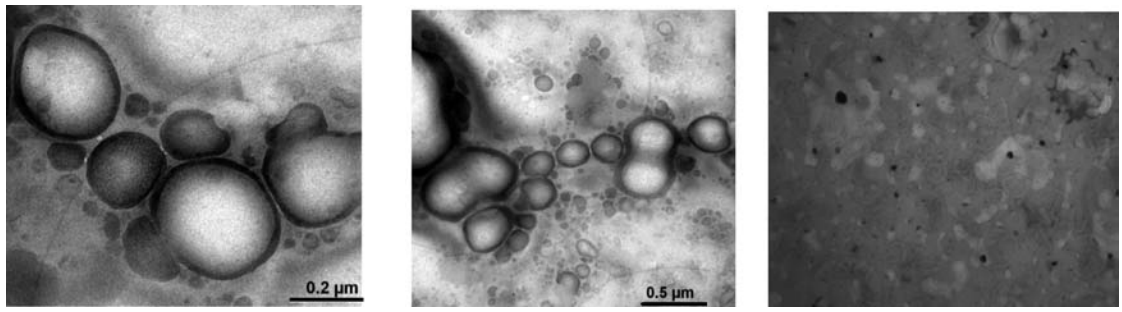

Figure 3. (a) TEM image of a representative vesicle from complex **1** in CH_2Cl_2 (1.0 mg/ml). (b) Formation of a fused vesicle at higher concentration (10.0 mg/ml). (c) TEM image of ruptured nanovesicles in CH_2Cl_2/CH_3CH_2OH.

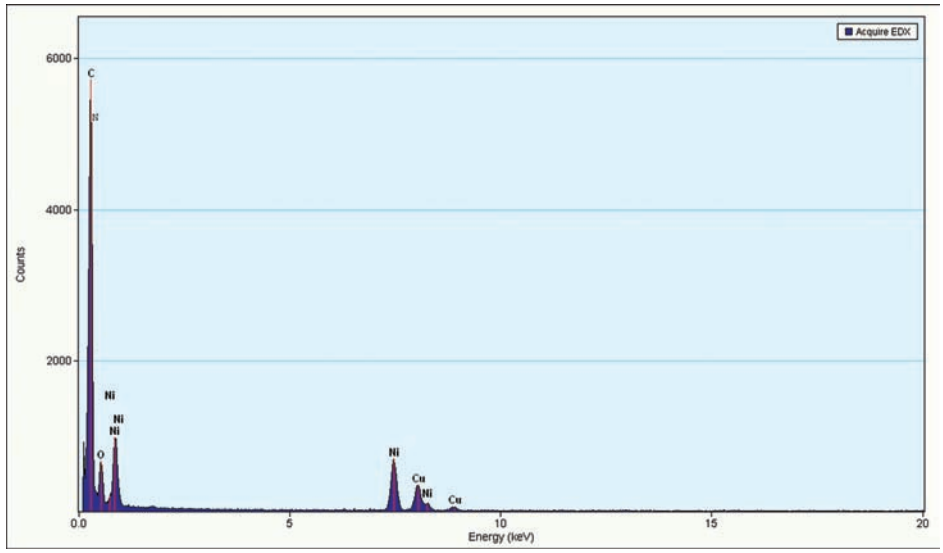

Figure 4. Selected area (surface) energy dispersive X-ray spectrum (EDS) pattern for **1** in CH_2Cl_2.

b axis. In a recent review,[20] it was shown that noncovalent interactions play a substantial role in the molecular assembly of Schiff base metal complexes and are also significant forces in the molecular recognition processes involving catalysts supported by Schiff base ligands.

Transmission Electron Microscopy and Scanning Electron Microscopy. TEM and SEM experiments were carried out to investigate the morphology of the complex **1** in CH_2Cl_2 medium. The TEM images revealed the formation of vesicles, with the diameters ranging from 280 to 300 nm (Figure 3a). Upon doing the same experiment with higher concentration of **1** in CH_2Cl_2 solution (10 mg/mL), gives fused vesicles (Figure 3b). In order to determine the local structure of the vesicle, an energy dispersive X-ray analysis (Figure 4) has been performed by selecting the vesicular wall, which clearly indicates that the vesicle walls are composed of Ni, C, N, and O, which come from the complex. Cu comes from the TEM grid. The selected area (surface) electron diffraction pattern (SAED) has also been shown in Figure S6 (Supporting Information). From SAED, it is clear that the vesicles are amorphous in nature. SEM images of the same sample (Figure 5) also reveal the exclusive formation of vesicles.

Atomic Force Microscopic Studies. Inspired by TEM and SEM experiments, we further studied AFM analysis in order to get an independent indication about the 3-D topography of the vesicular structure. A sample was prepared using a CH_2Cl_2 solution (3 mg/mL) on a mica foil by slow evaporation and vacuum drying at 30 °C for 2 days. The AFM analysis clearly confirmed the vesicular and fused vesicular configuration of the complex in CH_2Cl_2 (Figure 6a and 6b).

Dynamic Light Scattering Experiment. A DLS experiment was carried out to measure the size distribution of vesicles of complex **1** in CH_2Cl_2 (Figure 7). We found that the vesicles have a mean-square radius of gyration (*z* average) of 280 nm and a hydrodynamic diameter of 282 nm, and they show a polydispersity index (fractional dispersity) of 0.314. The mean-square radius of gyration value in the higher region indicates aggregation of the small vesicles into a larger one, which is in accordance with the fused vesicles as obtained in TEM and AFM images (Figures 3b and 6b). Thus, the DLS results correlated well with the TEM and AFM images. The DLS studies along with the microscopic studies clearly suggest the self-assembly of the Ni_3−Schiff base complex into vesicular structures in a CH_2Cl_2 medium.

(20) Lewi'nskia, J.; Zacharaa, J.; Justyniakb, I.; Drankaa, M. *Coord. Chem. Rev.* **2005**, *249*, 1185–1199.

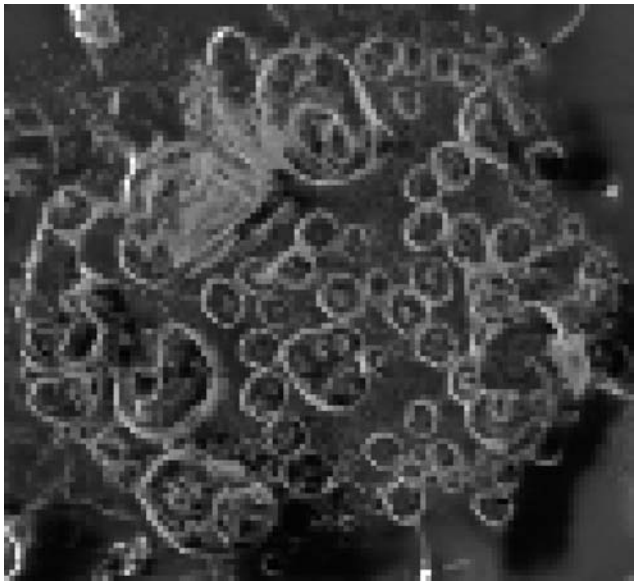

Figure 5. Scanning electron micrograph of vesicles in CH_2Cl_2.

Formation of Vesicles from the Sheet Structure and Rupture of It. It is evident from the TEM, SEM, and AFM images of complex **1** that the self-assembling molecule indeed forms vesicular structures in CH_2Cl_2 with a mean diameter of 290 nm. The formation of such vesicles may be envisaged by considering the closure of the supramolecular sheet-like structure in two different directions simultaneously, as illustrated in Scheme 1. However, the exact mechanisms for the formation of such vesicles are yet to be explored.

To clarify the driving force for such self-assembly and the stability of the vesicular structure, we have performed TEM experiments in some other organic solvent mixtures, for example, CH_2Cl_2/EtOH and CH_2Cl_2/CH_3CN. Surprisingly, it was found that the vesicular structure is not formed (Figure 3c) in these solvents. From these observations, it seems that there may be some role for the CH_2Cl_2 solvent in the formation of such vesicles. Further, doing the same experiment with a higher concentration of CH_2Cl_2 solution (10 mg/mL) gives fused vesicles (Figure 3b). The driving force behind the fusion process may be the release of strain in the initially formed vesicles, which have a high curvature. By fusing into larger vesicles, the curvature energy decreases, thus leading to a thermodynamically more stable state.[21]

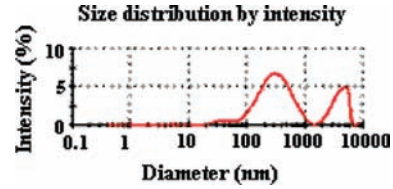

Figure 7. Size distribution profile of complex **1** through DLS study. Hydrodynamic diameter, 282 nm; polydispersity index, 0.314.

Scheme 1

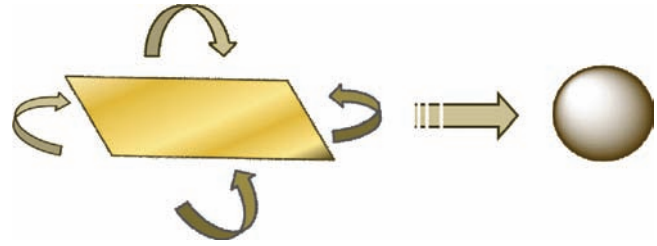

Encapsulation Studies. Entrapment of organic dye moecules such as methyl red within the vesicular structure has also been performed. When a CH_2Cl_2 solution of the methyl red dye is added into the CH_2Cl_2 solution of vesicles, the dye molecules are encapsulated. The confocal image of the encapsulated dye molecules is strong evidence of this phenomenon (Figure 8). This phenomenon has also been verified by comparing the absorption spectra of the free and encapsulated dye molecules (Figure 9). A mixture of a CH_2Cl_2 solution of complex **1** and methyl red in a 1:1 v/v ratio (the final concentration of each of the substances being 10^{-4} M) shows a significant decrease in the intensity of the absorption band of the dye compared to that of a 10^{-4} M solution of a pure dye (Figure 9). This clearly substantiates the entrapment of dye molecules in the vesicles. Interestingly, when CH_3CN or C_2H_5OH was added to this solution, all entrapped dye molecules got released, and the intensity of the absorption spectrum regained almost its initial value. The release of an entrapped dye molecule in CH_3CN or C_2H_5OH can be justified by the breakage of these vesicles, as shown in

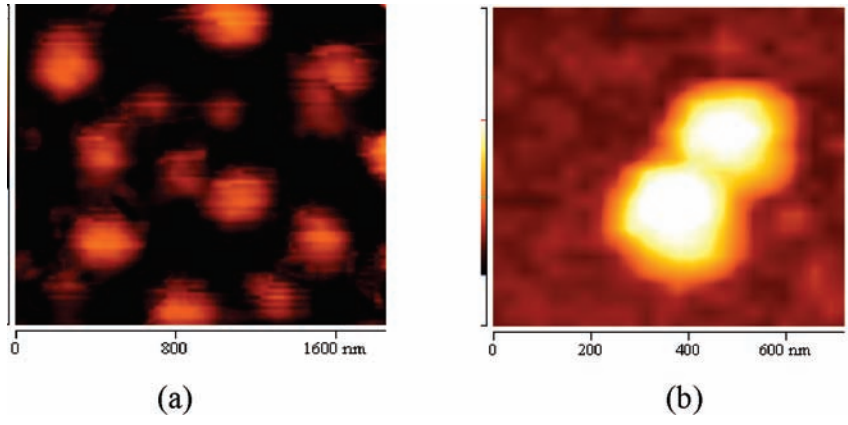

Figure 6. AFM topography image of a vesicle (a) and fused vesicles (b).

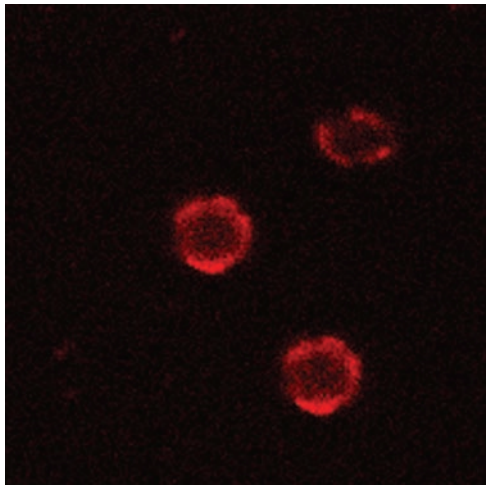

Figure 8. Confocal microscopic image showing the entrapment of dye, methyl red, by vesicles.

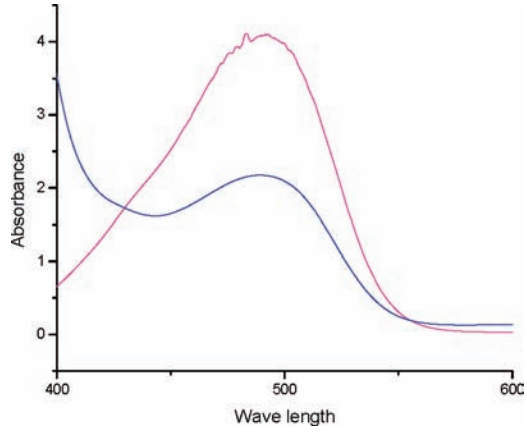

Figure 9. UV-absorption spectra showing the encapsulation and release of methyl red dye by vesicles in CH_2Cl_2. Purple curve indicates absorption spectra of dye; blue curve shows the absorption spectra of methyl red dye in the presence of vesicles.

Figure 3c. The phenomenon of rupturing of the vesicles by changing the solvent can potentially be utilized for the release of several organic dye or other organic-phase-soluble materials.

Conclusion

We demonstrate for the first time that a Schiff base complex of a transition metal can be self-assembled into unique supramolecular vesicular structures in solution. The nature of the vesicles can be adjusted by varying the concentration of the complex in solution. The absorption spectra before and after vesicle formation, the XPS, and the HRMS-ESI support the claim that the trinuclear nickel(II) complex is retained in CH_2Cl_2, that is, in the vesicle walls.

The vesicles are efficient at encapsulating organic dye molecules such as methyl red in a dichloromethane solution. On addition of other organic solvents, for example, acetonitrile or ethanol, to this solution, the vesicular structure of the complex is lost, and the dye is released. This suggests a tremendous scope for such metal-organic complex vesicles to act as a carrier for organic dye.

Acknowledgment. We thank CSIR, Government of India [Junior Research Fellowship to P.M., Sanction no. 09/028 (0663)/2006-EMR-I], EPSRC, and the University of Reading for funds for the X-Calibur system. We are also thankful to Prof. A. Dasgupta, University of Calcutta, for the DLS experiment and Dr. A. Banerjee, Indian Institute of Chemical Biology, for the confocal microscopy. We thank The Director, Central Glass and Ceramic Research Institute, for the permission for doing TEM experiments and K. Jithesh for the X-ray photoelectron spectra.

Supporting Information Available: Additional figures and tables. Crystallographic data in CIF format for the structure reported. This material is available free of charge via the Internet at http://pubs.acs.org.

IC801889A

(21) Lee, J.-K.; Lentz, B. R. *Biochemistry* **1997**, *36*, 6251–6257.